Epidermal Growth Factor Receptor (EGFR) Is Overexpressed in Anaplastic Thyroid Cancer, and the EGFR Inhibitor Gefitinib Inhibits the Growth of Anaplastic Thyroid Cancer

Bradley A. Schiff,[2] Andrea B. McMurphy,[2] Samar A. Jasser,[1] Maher N. Younes,[1] Dao Doan,[1] Orhan G. Yigitbasi,[1] Seungwon Kim,[1] Ge Zhou,[1] Mahitosh Mandal,[1] Benjamin N. Bekele,[3] F. Christopher Holsinger,[1] Steven I. Sherman,[4] Sai-Ching Yeung,[5] Adel K. El-Naggar,[1,6] and Jeffrey N. Myers[1,7]

Departments of [1]Head and Neck Surgery and [2]Otorhinolaryngology, Baylor College of Medicine, Houston, Texas; and Departments of [3]Biostatistics, [4]Endocrine Neoplasia and Hormonal Disorders, [5]Ambulatory Treatment and Emergency Care, [6]Pathology, and [7]Cancer Biology, The University of Texas M. D. Anderson Cancer Center, Houston, Texas

ABSTRACT

Purpose: No effective treatment options currently are available to patients with anaplastic thyroid cancer (ATC), resulting in high mortality rates. Epidermal growth factor (EGF) has been shown to play a role in the pathogenesis of many types of cancer, and its receptor (EGFR) provides an attractive target for molecular therapy.

Experimental Design: The expression of EGFR was determined in ATC *in vitro* and *in vivo* and in human tissue arrays of ATC. We assessed the potential of the EGFR inhibitor gefitinib ("Iressa," ZD1839) to inhibit EGFR activation *in vitro* and *in vivo*, inhibit ATC cellular proliferation, induce apoptosis, and reduce the growth of ATC cells *in vivo* when administered alone and in combination with paclitaxel.

Results: EGFR was overexpressed in ATC cell lines *in vitro* and *in vivo* and in human ATC specimens. Activation of EGFR by EGF was blocked by the addition of gefitinib. *In vitro* studies showed that gefitinib greatly inhibited cellular proliferation and induced apoptosis in ATC cell lines and slowed tumor growth in a nude mouse model of thyroid carcinoma cells injected subcutaneously.

Conclusions: ATC cells consistently overexpress EGFR, rendering this receptor a potential target for molecular therapy. Gefitinib effectively blocks activation of EGFR by EGF, inhibits ATC cellular proliferation, and induces apoptosis *in vitro*. Our *in vivo* results show that gefitinib has significant antitumor activity against ATC in a subcutaneous nude mouse tumor model and therefore is a potential candidate for human clinical trials.

INTRODUCTION

The annual prevalence of thyroid cancer in the United States was expected to be ~22,000 people in 2003 (1). The vast majority of thyroid carcinomas are differentiated and can often be cured surgically. Anaplastic thyroid carcinomas are relatively rare, constituting only 1.6% all of the thyroid cancers (2), and show extremely aggressive behavior, leading to a high mortality rate. Patients with anaplastic thyroid cancer (ATC) face a uniformly dismal prognosis, with average 5-year survival rates of <10% and a median survival time of 3 months (3). No effective treatment options currently are available to patients with ATC.

Targeted molecular therapy offers potential treatment alternatives for patients with ATC. Epidermal growth factor (EGF) and its receptor (EGFR) have been implicated in the pathogenesis of many different types of cancer and thus provide attractive targets for molecular therapy. EGFR, which is encoded by the c-*erb* proto-oncogene, is a M_r 170,000 transmembrane cell-surface glycoprotein consisting of an extracellular ligand binding domain, a transmembrane domain, and an intracellular domain with intrinsic tyrosine kinase activity (4, 5). Dimerization of EGFR following the binding of the ligand results in *trans*-phosphorylation of this receptor and subsequent activation of several downstream signal transduction pathways, including the mitogen-activated protein kinase and phosphatidylinositol-3′ kinase signaling pathways, which are involved in promoting cellular proliferation and survival (6–8). In preclinical studies, EGF has been shown to stimulate follicular cell proliferation and to enhance the migration and invasiveness of papillary thyroid cancer (9–11). The medical literature generally supports the concept that EGFR, although expressed at higher levels in anaplastic and papillary cancers than in normal thyroid tissue, is present in all of the thyroid tissues, but the data in different studies often vary widely (9, 12–17). In an *in vitro* study by Bergstrom *et al.* (18), EGFR was expressed in all six ATC cell lines examined, and constitutive phosphorylation of EGFR was found in three of the six cell lines tested.

High expression of EGFR appears to be a negative prognostic factor in multiple types of tumors, including breast cancer (19) and bladder cancer (20); however, few studies have examined the clinical implications of EGFR expression and location

Requests for reprints: Jeffrey N. Myers, Department of Head and Neck Surgery, Unit 441, The University of Texas M. D. Anderson Cancer Center, 1515 Holcombe Boulevard, Houston, TX 77030. Phone: 713-745-2667; Fax: 713-794-4662; E-mail: jmyers@mdanderson.org.

in thyroid cancer. A recent study found a statistically significant correlation between the staining intensity of EGF and recurrence of papillary thyroid cancer (16). In another report, cytoplasmic immunopositivity was significantly associated with the extent of primary tumor infiltration in papillary thyroid cancer, whereas membranous staining was not. Furthermore, in a multivariate survival analysis, strong cytoplasmic EGFR staining of papillary thyroid cancer was significantly associated with a decrease in recurrence-free survival (21). These findings suggest that the molecular blockage of EGFR activation has the potential to reduce thyroid tumor growth, making EGFR an attractive target for molecular therapy against ATC.

Gefitinib ("Iressa," ZD1839; AstraZeneca, Wilmington, DE), a synthetic anilinoquinazoline, is an orally active EGFR inhibitor that is highly selective, with minimal activity against other tyrosine kinases. Gefitinib has been shown to block EGF-stimulated EGFR autophosphorylation (22) and EGFR-mediated downstream signal transduction. The drug also has shown activity against a variety of human tumor cells *in vitro* and additive to synergistic effects when combined with radiation therapy or chemotherapy (23, 24). Results of Phase I trials have indicated that this agent offers good bioavailability and tolerability (25). Many Phase II and III studies currently are underway to assess the effectiveness of gefitinib against a variety of carcinomas, including breast, lung, colorectal, head and neck, prostate, and renal. Two recent studies have suggested that response to gefitinib therapy is linked to mutations in the *EGFR* gene (26, 27). Although numerous studies already have shown that gefitinib possesses clinically meaningful antitumor activity in several malignancies (28), to our knowledge, no clinical trials yet exist to determine the effectiveness of gefitinib against ATC. Thus, we investigated the role of EGFR and its inhibitor gefitinib in ATC to determine whether gefitinib possesses meaningful antitumor activity against ATC, potentially justifying clinical trials.

MATERIALS AND METHODS

Animals. Male athymic nude mice, ages 8 to 12 weeks, were purchased from the animal production area of the National Cancer Institute Frederick Cancer Research and Development Center (Frederick, MD). The mice were housed and maintained in laminar flow cabinets under specific pathogen-free conditions in facilities approved by the American Association for Accreditation of Laboratory Animal Care in accordance with current regulations and standards of the United States Department of Agriculture, the United States Department of Health and Human Services, and the NIH. The mice were treated in accordance with the Animal Care and Use Guidelines of the University of Texas M. D. Anderson Cancer Center (Houston, TX) under a protocol approved by the Institutional Animal Care Use Committee.

Cell Lines and Culture Conditions. The papillary thyroid carcinoma cell line NPA187 and the ATC cell lines KAT-4, K18, C643, HTH, ARO, and DRO were used. Oral cavity squamous cell cancer line TU167 was used as a positive control, and the fibroblast line 3T3 was used as a negative control. The cells were grown in Dulbecco's modified Eagle's medium supplemented with 10% fetal bovine serum (DMEM-10% FBS),

L-glutamine, penicillin, sodium pyruvate, nonessential amino acids, and a twofold vitamin solution (Life Technologies, Inc., Rockville, MD). Adherent monolayer cultures were maintained on plastic and incubated at 37°C in 5% carbon dioxide and 95% air. The cultures were free of *Mycoplasma* species. All of the cell lines injected into the mice tested free of the following pathogenic murine viruses: reovirus type 3, pneumonia virus, K virus, Theiler's encephalitis virus, Sendai virus, minute virus, ectromelia virus, and lactate dehydrogenase virus (as assayed by M.A. Bioproducts, Walkersville, MD). The cultures were maintained no longer than 12 weeks after recovery from frozen stocks.

Reagents. For *in vitro* administration, gefitinib was dissolved in dimethyl sulfoxide to a concentration of 20 mmol/L. For *in vivo* testing, gefitinib was dissolved in a lactate salt solution. Propidium iodide (PI) and tetrazolium (MTT) were purchased from Sigma-Aldrich Corp. (St. Louis, MO).

Western Immunoblot Analysis. All of the cells were incubated in serum-free medium for 24 hours. Cells were incubated with gefitinib for 1 hour at concentrations ranging from 0.01 to 100 μmol/L before addition of EGF (40 ng/mL) for 15 minutes. The cells then were washed with PBS, and lysis buffer was added [1% Triton X-100, 20 mmol/L Tris (pH 8.0), 137 mmol/L sodium chloride, 10% glycerol (v/v), 2 mmol/L EDTA, 1 mmol/L phenylmethylsulfonyl fluoride, 20 μmol/L aprotinin-leupeptin-trypsin inhibitor, and 2 mmol/L sodium orthovanadate]. The cells were scraped and spun in a centrifuge to remove insoluble proteins. The samples were diluted in sample buffer [10% SDS, 0.5 mmol/L Tris-HCl (pH 6.8), 1 mol/L dithiothreitol, 10% (v/v) glycerol, and 1% bromphenol blue] and boiled. The proteins (50 μg) were resolved on polyacrylamide gel electrophoresis and electrophoretically transferred onto 0.45-μg nitrocellulose membranes. The membranes were blocked with 5% (w/v) nonfat milk in 0.1% Tween 20 (v/v) in Tris-buffered saline, probed with rabbit monoclonal anti-EGFR (1:2000; Upstate Biotechnology, Inc., Lake Placid, NY) in 1% nonfat milk, and incubated with peroxidase-conjugated sheep antirabbit immunoglobulin (1:2000; Amersham, Piscataway, NJ) in 1% nonfat milk. The blots also were probed with rabbit anti–phospho-EGFR (p-EGFR 1068; Cell Signaling Technologies, Beverly, MA), diluted 1:1000 in 1% nonfat milk, and incubated with peroxidase-conjugated sheep antirabbit IgG (1:3000). All of the blots were probed with anti–β-actin (1:1000) in 1% nonfat milk, followed by horseradish peroxidase–conjugated donkey antirabbit IgG (1:2000; Amersham) in 1% nonfat milk. Protein bands were visualized using an enhanced chemiluminescence detection system (Amersham).

ELISA. Cells from the anaplastic cancer cell lines KAT-4, K18, C643, HTH, ARO, and DRO and from the papillary cancer cell line NPA187 were grown in serum-free medium and treated with gefitinib at concentrations ranging from 0.01 to 100 μmol/L. After 24 hours, the supernatant was collected, and the cells were counted. The supernatants were examined for transforming growth factor α (TGF-α) and EGF. All of the kits were purchased from R&D Systems (Minneapolis, MN), and all of the experiments were performed according to the manufacturer's instructions. The absorbance and concentration (pg/mL) were measured using a microplate reader at 450

nm. For each cell line, the results were plotted as the ratio of the concentration to the total number of cells.

PCR Analysis of EGFR Mutations. The PCR was used to amplify exons 18, 19, and 21 from the *EGFR* gene using genomic DNA isolated from the following tumor-derived cell lines: papillary thyroid cancer cell line NPA187 and ATC cell lines DRO, K18, ARO, HTH-74, C643, and KAT-4. PCR amplicons were purified using QIAquick PCR purification kit (Qiagen, Valencia CA) and then sent to LoneStar Labs (Houston, TX) for sequencing. Electropherograms were analyzed for the presence of mutations.

Measurement of Cell Proliferation. Gefitinib was tested on the KAT-4 ATC cell line using an MTT-based assay, which measures cell proliferation based on the ability of live cells to convert MTT to dark blue formazan. Two thousand cells were grown in DMEM-10% FBS, with and without 0.01 to 100 μmol/L gefitinib, in 96-well tissue culture plates. After 24 hours, the cells again were incubated with medium alone or medium containing various concentrations of gefitinib diluted in dimethyl sulfoxide. After a 3-day incubation, the number of metabolically active cells was determined by MTT assay using a 96-well microtiter plate reader (MR-5000; Dynatech Laboratories Inc., Chantilly, VA) at an absorbance of 570 nm. The absorbance for a control plate, which was not seeded with any cells during initial plating, was subtracted from the absorbance of every other well.

Measurement of Cell Death. Cells were plated at a density of 5×10^5 cells in 38 mm² six-well plates (Costar, Cambridge, MA) and maintained for 24 hours before treatment with gefitinib. After 24 hours, gefitinib was added at various concentrations. After treatment for 48 hours, PI staining of hypodiploid DNA determined the extent of cell death. A total of 3×10^5 cells were resuspended in a Nicoletti buffer [50 μg/mL PI, 0.1% sodium citrate, 0.1% Triton X-100, and 1 mg/mL RNase (Roche, Basel, Switzerland) in PBS] for 20 minutes at 4°C. Cells then were analyzed by flow cytometry, and the sub-G_0/G_1 fraction was measured using the Lysys software (Becton Dickinson, Franklin Lakes, NJ).

Immunohistochemical Analysis of Murine Tumor Frozen Sections and Human Tumor Tissue Arrays. Immunohistochemical analysis was performed using rabbit anti-EGFR antibodies (Santa Cruz Biotechnology, Santa Cruz, CA). Frozen tumors were sectioned (8 to 10 μm thick), mounted on positively charged Superfrost slides (Fisher Scientific, Houston, TX), air dried for 30 minutes, and fixed in cold acetone for 10 minutes. The slides were washed three times with PBS (pH 7.5), blocked for 20 minutes at room temperature in PBS supplemented with 1% normal goat serum and 5% normal horse serum (protein-blocking solution), and incubated with primary antibody for 18 hours at 4°C. Samples then were washed three times for 3 minutes, blocked with protein-blocking solution for 10 minutes, and incubated with AlexaFluor 594–conjugated goat antirabbit IgG (Molecular Probes, Eugene, OR) for 1 hour at room temperature in the dark. Samples again were washed three times for 5 minutes and then counterstained with 300 μg/mL Hoechst stain for 1 to 2 minutes at room temperature. The slides were washed again with PBS and then mounted using propyl gallate.

Immunofluorescence microscopy was performed in a Nikon Microphot-FXA (Nikon Inc., Tokyo, Japan) equipped with an HBO 100 mercury lamp and narrow bandpass filters to individually select for green, red, and blue fluorescence (Chroma Technology Corp., Brattleboro, VT). Images were captured using a cooled charge-coupled device Hamamatsu 5810 camera (Hamamatsu Corp., Bridgewater, NJ) and Optimas Image Analysis software (Media Cybernetics, Silver Spring, MD). Photomontages were prepared using Adobe Photoshop software (Adobe Systems Inc., San Jose, CA).

Human Thyroid Tissue Arrays. Thyroid tumor tissue arrays representative of the entire spectrum of benign and malignant neoplasms, including ATC constructed at the head and neck tissue care facility, were used to screen for EGFR expression. The arrays represented 14 papillary carcinomas, 6 anaplastic carcinomas, and 9 samples of nondiseased thyroid tissue. Two cores of each sample were placed differentially in the recipient block. Two pathologists scored these blindly and independently on a scale of 0 to 3. Whenever a discrepancy in scoring was noted, both pathologists reexamined the sample in question, and a consensus was reached.

***In vivo* Xenografts.** Tumor response to gefitinib was gauged using a nude mouse model of thyroid cancer. KAT-4 ATC cells were harvested from subconfluent cultures by trypsinization and then washed. Using a 30-gauge needle under direct visualization, 5×10^6 KAT-4 cells diluted in 30 μL of serum-free medium were injected subcutaneously into the cervical area. Tumors were allowed to grow for 14 days; all of the mice then were weighed, and all of the tumors were measured using microcalipers.

Tumor volume was calculated using the formula $(A)(B^2)\pi/6$, where A was the length of the longest aspect of the tumor, and B was the length of the tumor perpendicular to A. The two mice with the largest tumors and the three with the smallest tumors were excluded from the analysis. All of the other mice then were placed into groups of five mice with similar average tumor volumes. The groups then were randomized into seven treatment groups. Each mouse in group 1, the control group, received sodium lactate at a dosage of 0.2 mL/d for 5 days (Monday through Friday) for 2 weeks via oral gavage. All of the other groups received gefitinib dissolved in 0.2 mL of sodium lactate solution via oral gavage. The mice in group 2 each received 0.9 mg/d (30 mg/kg) for 5 days per week for 2 weeks; mice in group 3, 1.8 mg/d (60 mg/kg) for 5 days per week for 2 weeks; mice in group 4, 2.7 mg/d (90 mg/kg) for 5 days per week for 2 weeks; mice in group 5, 4.5 mg/d (150 mg/kg) for 5 days per week for 2 weeks; mice in group 6, 4.5 mg/d (150 mg/kg) for 5 days per week for 2 weeks + paclitaxel (200 μg/wk injected intraperitoneally); and mice in group 7, 4.5 mg/d (150 mg/kg) every other day (QOD), Monday, Wednesday, and Friday for 2 weeks. The mice were weighed and the tumors were measured on days 8 and 12 using microcalipers until the mice were euthanatized after 2 weeks of treatment. After the mice were euthanatized, the tumors again were measured, and the mice were weighed.

For immunohistochemical and routine hematoxylin and eosin staining, one part of the tissue was fixed in formalin and embedded in paraffin, and another part was embedded in optimal cutting-temperature compound (Miles Inc., Elkhart, IN),

Table 1 Level of staining for EGFR in normal, papillary, and anaplastic thyroid tissue from 29 human subjects

Tissue type	No. of subjects	EGFR staining				
		Level of staining				Percentage of specimen staining
		0	1	2	3	
Normal	9	9	0	0	0	0
Papillary	14	12	2	0	0	14
Anaplastic	6	1	3	2	0	83

Abbreviation: EGFR, epidermal growth factor receptor.

rapidly frozen in liquid nitrogen, and stored at −80°C. Hematoxylin and eosin staining confirmed the presence of tumors.

Statistical Analyses. To examine the results of EGFR in human thyroid tissue arrays, we performed three pairwise comparisons using Fisher's exact test. In the first analysis, the type I error rate was controlled at 0.017, guaranteeing that the overall type I error rate would be controlled at 0.05. To determine the IC_{50} for MTT and apoptosis assays, linear interpolation was used. We chose this method because the changes in absorbance as a percentage of the control and in apoptosis were linearly related to gefitinib levels in the range of the IC_{50}.

Two methods were used to analyze the data from the study involving the model in which nude mice were injected subcutaneously. The purpose of this analysis was to determine whether there was a statistically significant difference in change in tumor size between mice treated with gefitinib at dosages of 30, 60, 90, and 150 mg/d, 150 mg/d plus paclitaxel, and the control group. The endpoint of interest was the percentage change from initial tumor size at day 12 of treatment. The Wilcoxon rank sum test was used to detect statistical significance in the percentage change in tumor size from the initial tumor size at day 12. The Jonckheere-Terpstra test was used to test for evidence of a trend of decreasing tumor size with increasing treatment dosage.

RESULTS

Production of Growth Factors EGF and TGF-α by Thyroid Cancer Cell Lines. To assess whether ATC cells produce the EGFR ligands EGF and TGF-α, ELISA was used to assess their levels in culture supernatants from six anaplastic and one papillary cancer cell lines. EGF was not present at an appreciable level in the supernatants from any of the cell lines examined. TGF-α was present at a level of 38.5 pg/mL per cell number in the medium from the ATC cell line DRO but was not present at an appreciable level in any of the other cell lines examined.

Expression of EGFR in Human Tissue Arrays. To determine the expression level of EGFR in normal and neoplastic human thyroid tissue, tissue arrays of surgical specimens composed of normal thyroid tissue, papillary thyroid cancer, and ATC were obtained from Dr. Adel El-Naggar (Department of Surgical Pathology, M. D. Anderson Cancer Center). None of the nine normal tissue specimens stained positive for EGFR. Of the specimens from the 14 patients with papillary thyroid cancer, 2 stained positive for EGFR. Specimens from five of the six patients with ATC stained positive for EGFR; specimens from two of these five patients stained at level 2, whereas specimens from the three other patients stained at level 1. Comparisons of ATC specimens with normal thyroid tissue specimens and ATC specimens with papillary thyroid cancer specimens revealed statistically significant differences in EGFR expression ($P = 0.002$ and $P = 0.007$, respectively). No statistically significant difference in EGFR expression was found between the papillary thyroid cancer and the normal thyroid tissue specimens ($P = 0.5$; Table 1, Fig. 1).

Expression of EGFR/Phospho-EGFR in Human Thyroid Cancer Cell Lines. To assess expression of EGFR and p-EGFR in human thyroid tissue cell lines *in vitro*, Western blot analysis was performed on cellular lysates of the six ATC cell lines (ARO, C643, DRO, HTH, K18, and KAT-4) and the papillary cell line (NPA187). Five of the six ATC cell lines (all
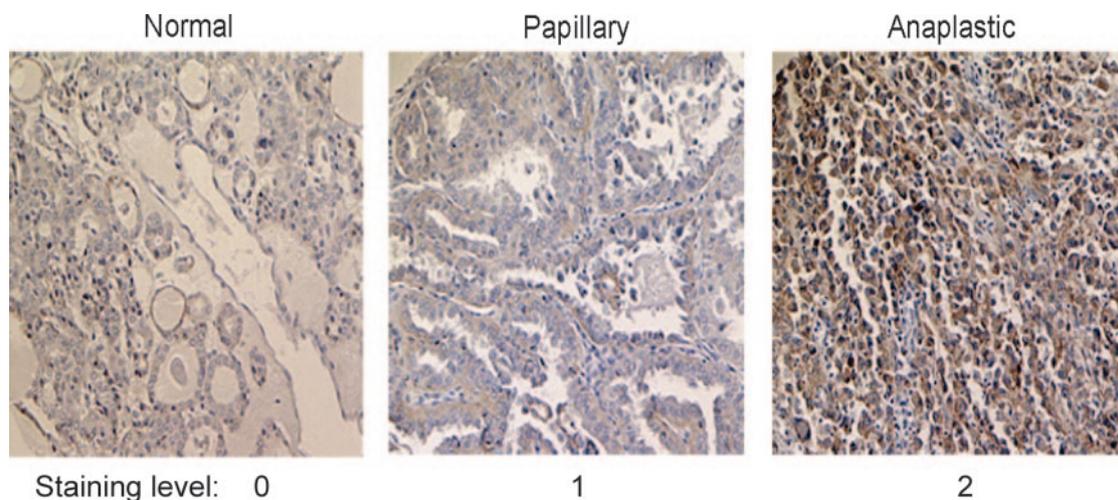
Fig. 1 Representative samples of the tissue arrays for normal thyroid tissue, papillary thyroid cancer, and ATC after staining for EGFR. Staining levels were 0, 1, and 2, respectively.
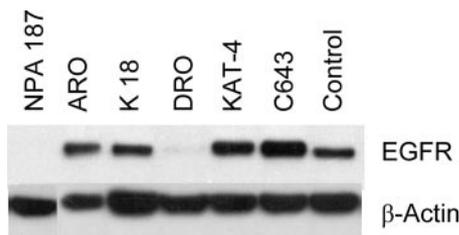
Fig. 2 Western blot analysis of cellular lysates of six ATC cell lines (ARO, C643, DRO, K18, and KAT-4) and the papillary cell line NPA187. Five of the six ATC cell lines (all except DRO) stained positive for EGFR, whereas NPA187 was negative for EGFR.

except DRO) stained positive for EGFR (Fig. 2), and the papillary cell line, NPA187, was negative for EGFR. In additional Western blot analyses, all of the cell lines were negative for the activated, or phosphorylated, form of EGFR (p-EGFR) unless stimulated with EGF (data not shown).

***In vivo* Expression of EGF, EGFR, and p-EGFR.** A nude mouse model was used to determine the expression of EGF, EGFR, and p-EGFR in mice implanted subcutaneously with 2.5×10^6 cells of KAT-4 ATC. Tumors were allowed to form, and after 1 month, the mice were euthanized, and the tumors were subjected to immunohistochemical staining. Normal murine thyroid tissue and ATC implants expressed EGFR and p-EGFR.

PCR Analysis of EGFR Showed No Mutations. Analysis of exons 18, 19, and 21 of EGFR showed no mutations in the six ATC cell lines tested (DRO, K18, ARO, HTH-74, C643, and KAT-4) or the papillary cell line NPA187.

Gefitinib Inhibited EGFR Phosphorylation in KAT-4 Cells *In vitro*. To assess whether gefitinib could inhibit EGFR signaling in ATC *in vivo*, KAT-4 ATC cell lines were exposed to serum-free medium for 24 hours. The cells then were treated with various concentrations of gefitinib in serum-free medium for 1 hour. The level of gefitinib ranged from 0.01 to 100 μmol/L. After 1 hour of exposure, recombinant EGF at a dosage of 40 ng/mL was added for 15 minutes. In Western blot analysis, the KAT-4 cells showed a high level of p-EGFR when stimulated with EGF. Gefitinib partially blocked EGF autophosphorylation of EGFR at a concentration of 0.01 μmol/L and almost completely blocked autophosphorylation at 1 μmol/L. At a concentration of 10 μmol/L, gefitinib completely blocked EGFR autophosphorylation (Fig. 3).

Gefitinib Inhibited EGFR Phosphorylation in KAT-4 Cells *In vivo*. To assess the efficacy of gefitinib inhibition of autophosphorylation of EGFR in ATC cells *in vivo*, mice implanted subcutaneously with the KAT-4 ATC cell line, which expresses a high level of p-EGFR, were treated with gefitinib at dosages of 30, 60, 90, and 150 mg/kg/d and at a dosage of 150 mg/kg/QOD. The mice treated with gefitinib at 30 and 60 mg/kg/d showed high levels of p-EGFR. The tumor sections from the mice treated with gefitinib at 90 mg/kg/d showed high levels of p-EGFR but lower expression than in tumor sections from the mice treated with 30 or 60 mg/kg/d. The mice treated with gefitinib at 150 mg/kg/QOD showed p-EGFR expression if they were euthanized immediately before the final treatment

but did not express p-EGFR if euthanized 6 hours after the final treatment. The mice treated with gefitinib at a dosage of 150 mg/kg/d showed no expression of p-EGFR, whether euthanized either immediately before or 6 hours after the final treatment (Fig. 4).

Gefitinib Inhibited Cellular Proliferation of KAT-4 Cells *In vitro*. To determine the effect of inhibition of EGFR signaling on ATC cell proliferation *in vitro*, three MTT assays were performed using gefitinib at concentrations ranging from 1 to 20 μmol/L (Fig. 5). The lowest concentration at which cellular proliferation was inhibited was 6 μmol/L. The IC_{50} was 8.36 μmol/L, and maximal inhibition occurred at a concentration of 14 μmol/L.

Gefitinib Induced Apoptosis in KAT-4 Cells *In vitro*. To assess the effects of gefitinib on induction of cell death of ATC cells, we performed a PI apoptosis assay on KAT-4 cells after 48 hours of treatment. When treated at a concentration of 8 μmol/L (the IC_{50} for the MTT assays), 5.5% of the cells underwent apoptosis. At a concentration of 12 μmol/L, 27.6% of the cells were apoptotic; at 19 μmol/L, 54.7%; at 22 μmol/L, 80.7%; and at 50 μmol/L, 94.5% (Fig. 6). The estimated IC_{50} for the apoptosis assays was 18.35 μmol/L.

Gefitinib Alone and in Combination with Paclitaxel Reduced KAT-4 Tumor Size and Growth in a Nude Mouse Model of Thyroid Cancer. A nude mouse model of thyroid cancer was used for the *in vivo* portion of the study to assess the *in vivo* antitumor activity of gefitinib. At day 12, the control group of mice showed an increased tumor size of 173% of the initial tumor size. The groups treated with gefitinib at dosages of 30, 60, 90, and 150 mg/kg/d had increased tumor sizes at day 12 of 158%, 165%, 112%, and 104% of the initial tumor size, respectively. The group treated with paclitaxel alone had an increase in tumor size at day 12 of 134% of initial tumor size. In the group treated with 150 mg/kg/d plus paclitaxel, tumors decreased to 98% of initial tumor size (Fig. 7).

DISCUSSION

Because patients with ATC face a dismal prognosis and have no effective treatment options, novel treatments are needed. The EGFR is involved in the pathogenesis or progression of many different types of cancers and therefore is a potential target for molecular therapy in ATC. However, little
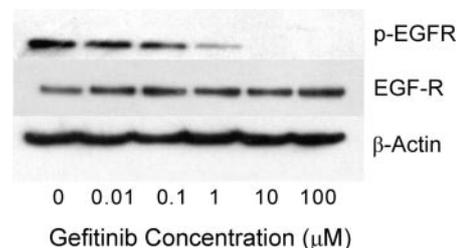

Fig. 3 Western blot analysis of KAT-4 ATC cell lines treated with various concentrations of gefitinib and subsequently exposed to EGF. Gefitinib partially blocked EGF autophosphorylation of EGFR at a concentration of 0.01 μmol/L and almost completely blocked autophosphorylation at 1 μmol/L. At a concentration of 10 μmol/L, gefitinib completely blocked EGFR autophosphorylation.
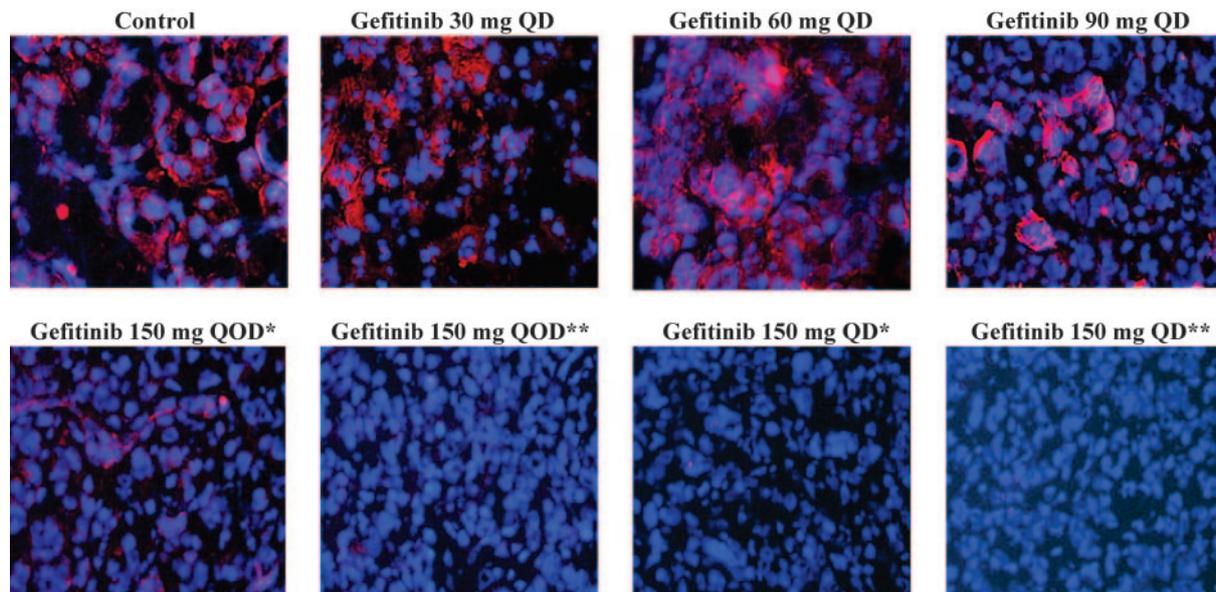
Fig. 4 Immunohistochemical results of mice subcutaneously implanted with KAT-4 ATC cell line and treated with various dosages of gefitinib. The tumors of mice treated with 30 and 60 mg/kg QD (*QD,* every day) of gefitinib showed high levels of p-EGFR, whereas the tumors of mice treated with 90 mg/kg/d showed lower expression of p-EGFR. The tumors of mice treated with 150 mg/kg QOD (*QOD,* every other day) showed p-EGFR expression if the mice were euthanatized immediately before the final treatment with gefitinib (48 hours after the previous gefitinib treatment) but did not express p-EGFR if sacrificed 6 hours after the final treatment. The tumors of mice treated with 150 mg/kg/d of gefitinib showed no expression of p-EGFR whether the mice were euthanatized either immediately before or 6 hours after the final treatment with gefitinib. This showed that gefitinib at a dosage of 150 mg/kg/d can completely block expression of p-EGFR in a nude mouse model of thyroid carcinoma. * Killed immediately before treatment. ** Killed 6 hours after treatment.

research has been done to examine the role of EGFR in ATC and the effectiveness of anti-EGFR therapies against ATC. Gefitinib is an EGFR tyrosine kinase inhibitor that has already been shown to have a favorable safety and tolerability profile in numerous Phase I clinical trials and therefore is a promising area of investigation in the search for effective treatments for patients with ATC.

To initiate studies, we performed ELISA to determine the expression of growth factors TGF-α and EGF. EGF was not present in any of the six ATC cell lines examined, and TGF-α was present only in the DRO cell line. DRO, the only ATC cell line that did not express EGFR, also was the only tested cell line that expressed TGF-α. In papillary thyroid cancer, TGF-α and EGFR expression often are linked.

Our thyroid tissue arrays showed significantly greater EGFR expression in ATC specimens than in either normal thyroid tissue or papillary thyroid cancer specimens ($P = 0.002$ and 0.007, respectively). The medical literature on this topic is mixed. Some studies (29) report that EGFR is expressed only in diseased thyroid tissue, whereas others report that EGFR is expressed in all of the thyroid tissues (9). However, most studies suggest that EGFR is expressed at a higher level in thyroid cancer than in normal thyroid tissue (30, 31). The data from our tissue arrays support this finding and suggest that EGFR is highly expressed in ATC.

Our analysis of the expression of EGFR by Western blot analysis showed no expression of EGFR in the papillary cell line NPA187 but did show EGFR expression in five of the six ATC
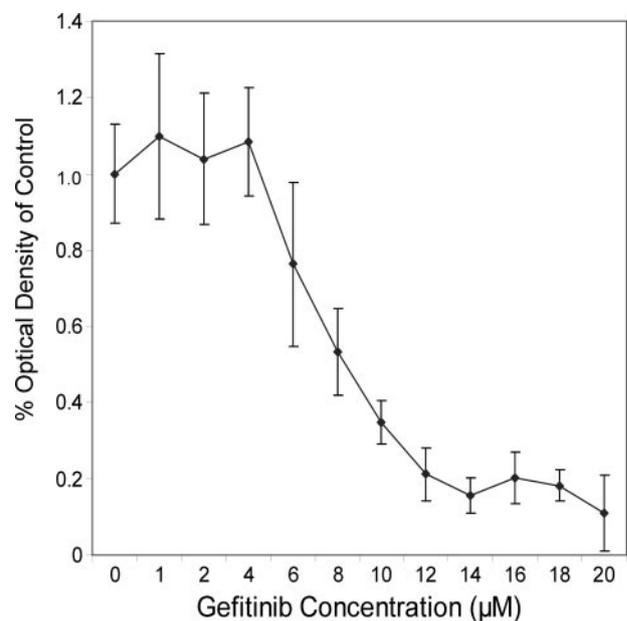
Fig. 5 MTT assay of KAT-4 ATC cells exposed to various concentrations of gefitinib. The lowest concentration at which cellular proliferation was inhibited was 6 μmol/L, and the IC$_{50}$ was 8.36 μmol/L. Maximal inhibition occurred at a concentration of 14 μmol/L. Thus, gefitinib is able to effectively inhibit ATC cellular proliferation.
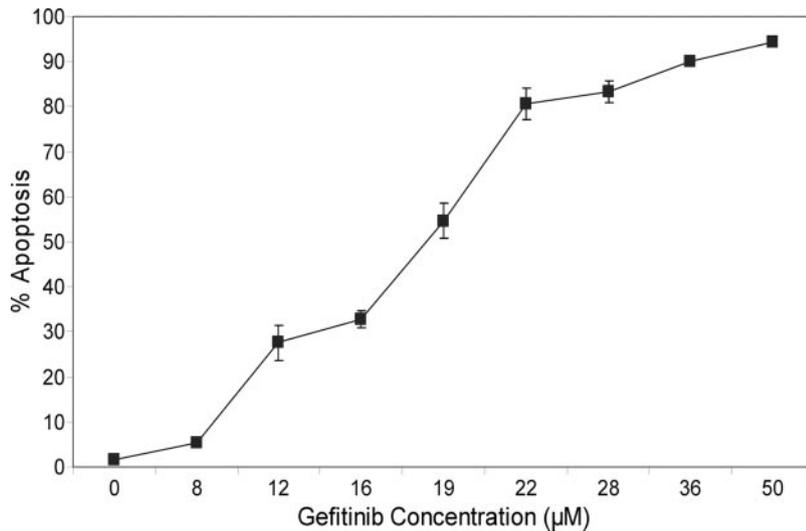
Fig. 6 PI apoptosis assay on KAT-4 cells after 48 hours of treatment with gefitinib. When treated at a concentration of 8 μmol/L (the IC$_{50}$ for the MTT assays), 5.5% of the cells underwent apoptosis. The estimated IC$_{50}$ for the apoptosis assays was 18.4 μmol/L. At a gefitinib concentration of 22 μmol/L, 80.7% of cells underwent apoptosis, whereas at 50 μmol/L, 94.5% of cells underwent apoptosis. This shows that gefitinib is able to induce apoptosis in ATC cell lines.

cell lines. The results also showed that EGFR was not constitutively phosphorylated in any of the ATC cell lines tested, but EGFR phosphorylation was readily observed in these cell lines after stimulation with EGF. These data are in concordance with those from previous studies that suggest that EGFR is expressed in ATC cell lines, but they contradict the literature that suggests that EGFR is constitutively activated in some ATC cell lines. However, immunohistochemical staining of sections of subcutaneously implanted KAT-4 tumors revealed that those tumors constitutively expressed EGFR and p-EGFR, as did normal murine thyroid tissue, suggesting that EGFR activation is upregulated *in vivo*.

We also showed that gefitinib blocked EGF-mediated activation of EGFR on ATC cell lines *in vitro*. The mice treated with 30 and 60 mg/kg/d of gefitinib showed high levels of p-EGFR. Specimens from the mice treated with 90 mg/kg/d of gefitinib showed high levels of p-EGFR but did not stain as positively as did those from the mice treated with 30 or 60 mg/kg/d. The mice treated with gefitinib 150 mg/kg/d showed no expression of p-EGFR regardless of whether they were euthanatized 6 hours after the final treatment or immediately before the final treatment was scheduled, a fact that indicates that gefitinib at a dosage of 150 mg/kg/d is able to continuously suppress EGFR phosphorylation. The mice treated with 150
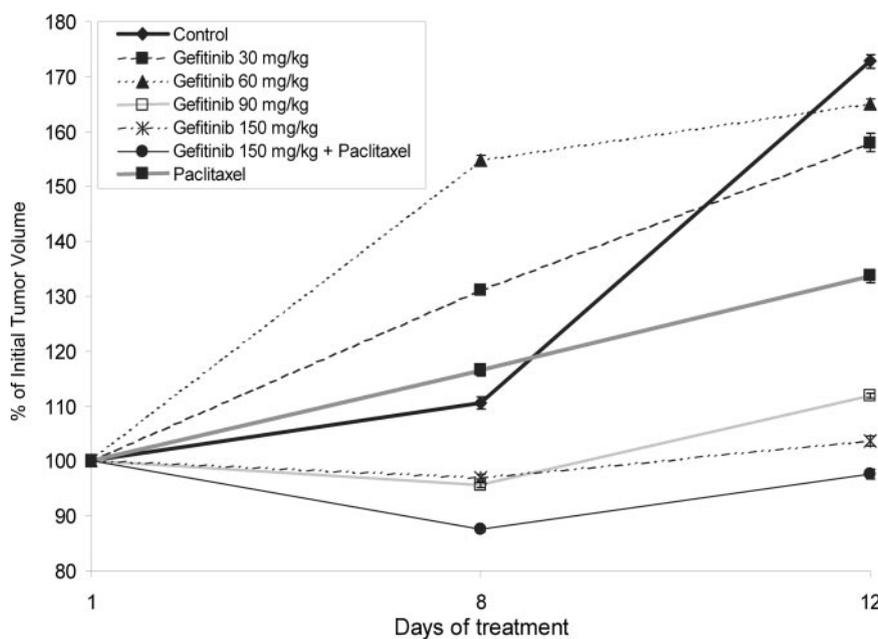

Fig. 7 A nude mouse model of thyroid carcinoma cells injected subcutaneously was used to assess the *in vivo* antitumor activity of gefitinib. At day 12, the control group of mice showed an increased tumor size of 173% of the initial tumor size. The groups treated with gefitinib at dosages of 30, 60, 90, and 150 mg/kg/d had increased tumor sizes at day 12 of 158%, 165%, 112%, and 104% of the initial tumor size, respectively. The group treated with paclitaxel alone had an increase in tumor size at day 12 of 134% of initial tumor size. In the group treated daily with 150 mg/kg/d gefitinib + paclitaxel, tumors decreased to 98% of initial tumor size. This shows that gefitinib, alone and in combination with paclitaxel, was able to reduce the growth of ATC in a nude mouse model of thyroid carcinoma cells injected subcutaneously.

mg/kg/QOD of gefitinib showed p-EGFR expression if euthanatized immediately before the final treatment was supposed to be given but did not express p-EGFR if euthanatized 6 hours after the final treatment, showing that a dosage of 150 mg/kg is unable to suppress EGFR phosphorylation for 48 hours. Our data show that gefitinib at a daily dosage of 150 mg/kg is able to suppress EGFR activation for 24 to 48 hours in a nude mouse model of thyroid cancer.

After establishing that EGFR is overexpressed in ATC and that gefitinib can suppress EGFR phosphorylation *in vitro* and *in vivo*, we then examined the effect of gefitinib on ATC cell growth and death. An MTT assay showed that 12 μmol/L of gefitinib caused near-total growth inhibition. A PI apoptosis assay revealed that 22 μmol/L of gefitinib induced a rate of apoptosis >80%. Thus, gefitinib is able to effectively inhibit ATC cellular proliferation and induce apoptosis in ATC cell lines, providing further evidence that gefitinib is effective against ATC.

The final portion of our experiments used a nude mouse model to examine the effects of various dosing schedules of gefitinib alone or in combination with paclitaxel on subcutaneously implanted KAT-4 tumors. The difference in change in tumor size between the control group and the group treated with gefitinib at a dosage of 150 mg/d + paclitaxel approached but did not achieve statistical significance ($P = 0.06$). However, if a trend analysis is done looking at increasing doses of gefitinib (and including gefitinib 150 mg/d + paclitaxel as the group receiving the highest level of treatment), there is a significant difference between change in tumor size and increasing treatment dosage ($P = 0.015$).

In summary, EGF has been shown to play a role in the pathogenesis of many types of cancer, and its receptor provides a promising target for molecular therapy. Little research has been done to examine the role of EGFR in ATC. Novel treatment strategies are needed for patients with ATC because current treatment options offer little benefit. We showed that EGFR is increased in ATC cell lines *in vitro* and *in vivo* and in human ATCs. Gefitinib was able to inhibit EGFR phosphorylation *in vitro* and *in vivo* and to reduce cellular proliferation and induce apoptosis in ATC cell lines. Finally, gefitinib alone and in combination with paclitaxel was able to reduce the growth of ATC cells in a nude mouse model of thyroid carcinoma cells injected subcutaneously. The favorable safety profile of gefitinib has already been proven in Phase I clinical trials, and based on the data presented here, clinical trials of gefitinib in patients with ATC are warranted.

REFERENCES

1. Jemal A, Murray T, Samuels A, Ghafoor A, Ward E, Thun MJ. Cancer statistics, 2003. CA Cancer J Clin 2003;53:5–26.

2. Gilliland FD, Hunt WC, Morris DM, Key CR. Prognostic factors for thyroid carcinoma. A population-based study of 15,698 cases from the Surveillance, Epidemiology and End Results (SEER) program 1973–1991. Cancer 1997;79:564–73.

3. McIver B, Hay ID, Giuffrida DF, et al. Anaplastic thyroid carcinoma: a 50-year experience at a single institution. Surgery 2001;130:1028–34.

4. Ullrich A, Coussens L, Hayflick JS, et al. Human epidermal growth factor receptor cDNA sequence and aberrant expression of the amplified gene in A431 epidermoid carcinoma cells. Nature 1984;309:418–25.

5. Carpenter G, Cohen S. Epidermal growth factor. J Biol Chem 1990;265:7709–12.

6. Ullrich A, Schlessinger J. Signal transduction by receptors with tyrosine kinase activity. Cell 1990;61:203–12.

7. Aaronson SA. Growth factors and cancer. Science 1991;254:1146–53.

8. Marti U, Ruchti C, Kampf J, et al. Nuclear localization of epidermal growth factor and epidermal growth factor receptors in human thyroid tissues. Thyroid 2001;11:137–45.

9. van der Laan BF, Freeman JL, Asa SL. Expression of growth factors and growth factor receptors in normal and tumorous human thyroid tissues. Thyroid 1995;5:67–73.

10. Hoelting T, Siperstein AE, Clark OH, Duh QY. Epidermal growth factor enhances proliferation, migration, and invasion of follicular and papillary thyroid cancer in vitro and in vivo. J Clin Endocrinol Metab 1994;79:401–8.

11. Bechtner G, Schopohl D, Rafferzeder M, Gartner R, Welsch U. Stimulation of thyroid cell proliferation by epidermal growth factor is different from cell growth induced by thyrotropin or insulin-like growth factor I. Eur J Endocrinol 1996;134:639–48.

12. Lemoine NR, Hughes CM, Gullick WJ, Brown CL, Wynford-Thomas D. Abnormalities of the EGF receptor system in human thyroid neoplasia. Int J Cancer 1991;49:558–61.

13. Westermark K, Lundqvist M, Wallin G, et al. EGF-receptors in human normal and pathological thyroid tissue. Histopathology 1996;28:221–7.

14. Duh QY, Gum ET, Gerend PL, Raper SE, Clark OH. Epidermal growth factor receptors in normal and neoplastic thyroid tissue. Surgery 1985;98:1000–7.

15. Duh QY, Siperstein AE, Miller RA, Sancho JJ, Demeure MJ, Clark OH. Epidermal growth factor receptors and adenylate cyclase activity in human thyroid tissues. World J Surg 1990;4:410–8.

16. Mizukami Y, Nonomura A, Hashimoto T, et al. Immunohistochemical demonstration of epidermal growth factor and c-myc oncogene product in normal, benign and malignant thyroid tissues. Histopathology 1991;18:11–8.

17. Aasland R, Akslen LA, Varhaug JE, Lillehaug JR. Co-expression of the genes encoding transforming growth factor-α and its receptor in papillary carcinomas of the thyroid. Int J Cancer 1990;46:382–7.

18. Bergström JD, Westermark B, Heldin N-E. Epidermal growth factor receptor signaling activates Met in human anaplastic thyroid carcinoma cells. Exp Cell Res 2000;259:293–9.

19. Nicholson S, Richard J, Sainsbury C, et al. Epidermal growth factor receptor (EGFr); results of a 6 year follow-up study in operable breast cancer with emphasis on the node negative subgroup. Br J Cancer 1991;63:146–50.

20. Lipponen P, Eskelinen M. Expression of epidermal growth factor receptor in bladder cancer as related to established prognostic factors, oncoprotein (c-erbB-2, p53) expression and long-term prognosis. Br J Cancer 1994;69:1120–5.

21. Akslen LA, Myking AO, Salvesen H, Varhaug JE. Prognostic impact of EGF-receptor in papillary thyroid carcinoma. Br J Cancer 1993;68:808–12.

22. Wakeling AE, Guy SP, Woodburn JR, et al. ZD1839 (Iressa): an orally active inhibitor of epidermal growth factor signaling with potential for cancer therapy. Cancer Res 2202;62:5749–54.

23. Ciardiello F. EGFR-targeted agents potentiate the antitumour activity of chemotherapy and radiotherapy. Signal 2002;2:4–11.

24. Sirotnak FM, Zakowski MF, Miller VA, Scher HI, Kris MG. Efficacy of cytotoxic agents against human tumor xenographs is markedly enhanced by coadministration of ZD1839 (Iressa), an inhibitor of EGFR tyrosine kinase. Clin Cancer Res 2000;6:4885–92.

25. Ranson M. ZD1839 (Iressa): for more than just non-small cell lung cancer. Oncologist 2002;7(Suppl 4):16–24.

26. Lynch TJ, Bell DW, Sordella R, et al. Activating mutations in the epidermal growth factor receptor underlying responsiveness of non-small-cell lung cancer to gefitinib. N Engl J Med 2004;350: 2129–39.

27. Paez JG, Jänne PA, Lee JC, et al. *EGFR* mutations in lung cancer: correlation with clinical response to gefitinib therapy. Science 2004; 304:1497–500.

28. Herbst RS. ZD1839: targeting the epidermal growth factor receptor in cancer therapy. Expert Opin Investig Drugs 2002;11:837–49.

29. Haugen DR, Akslen LA, Varhaug JE, Lillehaug JR. Demonstration of a TGF-α-EGF-receptor autocrine loop and c-myc protein over-expression in papillary thyroid carcinomas. Int J Cancer 1993;55:37–43.

30. Aasland R, Akslen LA, Varhaug JE, Lillehaug JR. Co-expression of the genes encoding transforming growth factor-α and its receptor in papillary carcinomas of the thyroid. Int J Cancer 1990;46:382–7.

31. Gorgoulis V, Aninos D, Priftis C, et al. Expression of epidermal growth factor, transforming growth factor-α and epidermal growth factor receptor in thyroid tumors. In Vivo 1992;6:291–6.